Applied Radiation and Isotopes 83 (2014) 109–114

Contents lists available at ScienceDirect

Applied Radiation and Isotopes

journal homepage: www.elsevier.com/locate/apradiso

# A study of the energy deposition profile of proton beams in materials of hadron therapeutic interest

Rafael Garcia-Molina [a,*], Isabel Abril [b], Pablo de Vera [b], Ioanna Kyriakou [c], Dimitris Emfietzoglou [c]

[a] Departamento de Física, Centro de Investigación en Óptica y Nanofísica, Universidad de Murcia, E-30100 Murcia, Spain
[b] Departament de Física Aplicada, Universitat d'Alacant, E-03100 Alacant, Spain
[c] Medical Physics Laboratory, University of Ioannina Medical School, GR-45110 Ioannina, Greece

## HIGHLIGHTS

- The energy loss per unit path length by protons in liquid water, PMMA and polystyrene is calculated.
- We use a realistic description of the target excitation spectrum.
- Depth–dose curves of proton beams in these materials are obtained by using the simulation code SEICS.
- We obtain how the dose broadens radially as the depth increases.
- SEICS includes the main interaction phenomena between the projectile and the target constituents.

## ARTICLE INFO

Available online 14 January 2013

*Keywords:*
Hadron therapy
Proton beam
Bragg curve
Liquid water
Simulation
Depth–dose profile

## ABSTRACT

The energy delivered by a swift proton beam in materials of interest to hadron therapy (liquid water, polymethylmethacrylate or polystyrene) is investigated. An explicit condensed-state description of the target excitation spectrum based on the dielectric formalism is used to calculate the energy-loss rate of the beam in the irradiated materials. This magnitude is the main input in the simulation code SEICS (Simulation of Energetic Ions and Clusters through Solids) used to evaluate the dose as a function of the penetration depth and radial distance from the beam axis.



## 1. Introduction

The interaction of swift charged particles with different materials is currently used to gain insight into the structure of matter, as well as to characterize and modify the properties of the bombarded targets (Nastasi et al., 1998).

Besides the application to inert substances, the study of energetic projectiles interacting with materials of biological interest is also useful because they can be utilized in a controlled manner to kill malignant tumor cells, following the pioneering suggestion made by Wilson (1946).

The use of proton (or heavier ion) beams for treating tumors lies in the reduced amount of energy deposited into healthy tissue (as compared to photon or electron beam techniques) in contrast with the higher dose delivered at the tumor location, and the well defined range reached by the beam. Both characteristics are embodied in the depth–dose curve (commonly referred to as the Bragg curve), which represents the amount of energy delivered by the projectile as a function of the depth in the target.

Therefore, an accurate knowledge of the energy deposition profile (through the depth–dose curve and the spatial dispersion of the beam) is needed for an optimal application of treatment plannings in hadron therapy. It should be noticed that this is only the first step in a multiscale approach (Solov'yov et al., 2009) to a deeper understanding of the processes that are relevant for ion beam cancer therapy.

In Section 2 we summarize the formalism used to calculate, from the condensed matter point of view, the target stopping power and energy-loss straggling, which are the main features of the energy deposited by a proton beam in materials currently used in hadron therapy treatment planning, such as liquid water, polymethylmethacrylate (PMMA) or polystyrene (PS). These analytical results are employed in Section 3 as input into the simulation code SEICS, used to describe in detail the motion and the interactions of the beam particles through the bombarded target. In Section 4 we present and discuss our simulations for the

* Corresponding author. Fax: +34 868 888 568.
*E-mail address:* rgm@um.es (R. Garcia-Molina).

0969-8043/$ - see front matter © 2013 Elsevier Ltd. All rights reserved.
http://dx.doi.org/10.1016/j.apradiso.2013.01.006

dose delivered as a function of the penetration depth (the Bragg curve) and also the radial distance to the beam axis. Finally, the conclusions of our work are drawn in Section 5.

## 2. Dielectric formalism of the energy loss by charged projectiles

The dielectric formalism (Lindhard, 1954; Ritchie, 1959) provides simple expressions for the most relevant magnitudes describing the electronic energy loss of a fast projectile (with mass $M$ and charge state $Q$) moving through matter with kinetic energy $E$, namely the stopping power $S_Q$ and the energy loss straggling $\Omega_Q^2$:

$$S_Q(E)=\frac{e^2M}{\pi E}\int_0^{\infty}\frac{\mathrm{d}k}{k}\rho_Q^2(k)\int_0^{k\sqrt{2E/M}}d\omega\,\omega\mathrm{Im}\left[\frac{-1}{\varepsilon(k,\omega)}\right], \tag{1}$$

$$\Omega_Q^2(E)=\frac{e^2M\hbar}{\pi E}\int_0^{\infty}\frac{\mathrm{d}k}{k}\rho_Q^2(k)\int_0^{k\sqrt{2E/M}}d\omega\,\omega^2\mathrm{Im}\left[\frac{-1}{\varepsilon(k,\omega)}\right]. \tag{2}$$

The dependence upon the target properties is accounted for in these expressions through its energy-loss function (ELF) $\mathrm{Im}[-1/\varepsilon(k,\omega)]$, which is related to the probability that the projectile loses energy via an electronic excitation with momentum transfer $\hbar k$ and energy transfer $\hbar\omega$ to the target.

The projectile structure enters by means of the Fourier transform of its charge distribution, $\rho_Q(k)$, which is calculated according to the modified Brandt–Kitagawa model (Brandt and Kitagawa, 1982).

As a consequence of stochastic charge-exchange with the target electrons, the projectiles of a beam can be in different charge-states $Q$. Therefore, the stopping power $S$ and the energy-loss straggling $\Omega^2$ characterizing the energy lost by a beam of particles with atomic number $Z$ and with a given energy $E$ are expressed as a weighted sum over $S_Q(E)$ and $\Omega_Q^2(E)$, respectively,

$$S(E)=\sum_{Q=0}^{Z}\phi_Q(E)S_Q(E), \tag{3}$$

$$\Omega^2(E)=\sum_{Q=0}^{Z}\phi_Q(E)\Omega_Q^2(E), \tag{4}$$

where the charge-state fractions, $\phi_Q(E)$, which do not only depend on the projectile energy, but also on its nature as well as on the target characteristics, are obtained from a parameterization to the experimental equilibrium charge fractions (Schiwietz and Grande, 2001).

Among various semi-empirical computational schemes (Emfietzoglou et al., 2009; Garcia-Molina et al., 2012) for modeling the ELF, the MELF-GOS (Mermin Energy Loss Function-Generalized Oscillator Strength) method (Abril et al., 1998; Heredia-Avalos et al., 2005) yields a realistic description of the target excitation spectrum over the whole energy-momentum space for a broad range of materials (metals, insulators, semiconductors, and biomaterials), provided experimental optical data are available.

In this work we will be concerned with materials of biological interest, such as liquid water, PMMA and PS, which are frequently used in hadron therapy treatment plans as tissue phantoms. In Fig. 1 we show, by symbols, the experimental optical ELF ($k=0$) of liquid water (Hayashi et al., 2000), PMMA (Ritsko et al., 1978) and PS (Inagaki et al., 1977), where the corresponding fitting with the MELF-GOS model (lines) is also included. The MELF-GOS methodology makes a separation of the ELF into outer and inner electronic excitation contributions (Abril et al., 1998; Heredia-Avalos et al., 2005),

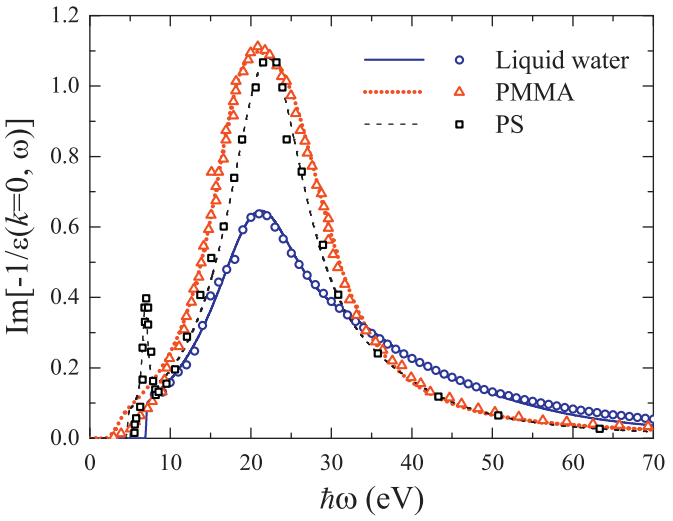


**Fig. 1.** Experimental energy loss function, $\mathrm{Im}[-1/\varepsilon(k=0,\omega)]$, of liquid water (circles) (Hayashi et al., 2000), PMMA (triangles) (Ritsko et al., 1978) and PS (squares) (Inagaki et al., 1977) in the optical limit ($k=0$). Lines correspond to the fit by the MELF-GOS model.

**Table 1**
Fitting parameters $A_i$, $\hbar\omega_i$ and $\hbar\gamma_i$ used in the MELF-GOS model for liquid water, PMMA and PS. $\hbar\omega_{\mathrm{th},i}$ is the threshold energy appearing in Eq.(5).

| Target | $i$ | $\hbar\omega_i$ (eV) | $\hbar\omega_i$ (eV) | $A_i$ | $\hbar\omega_{\mathrm{th},i}$(eV) |
|---|---|---|---|---|---|
| Liquid water | 1 | 22.0 | 14.00 | 0.23 | 7 |
| | 2 | 34.0 | 19.00 | 0.131 | |
| | 3 | 47.0 | 31.97 | 1.15 | |
| PMMA | 1 | 19.14 | 9.07 | 0.128 | 3 |
| | 2 | 25.36 | 14.41 | 0.395 | |
| | 3 | 70.75 | 48.98 | 0.030 | |
| PS | 1 | 6.88 | 0.68 | 0.002 | 4.6 |
| | 2 | 22.86 | 12.25 | 0.390 | |
| | 3 | 36.74 | 21.77 | 0.080 | |

$$\begin{aligned}\mathrm{Im}\left[\frac{-1}{\varepsilon(k,\omega)}\right]&=\mathrm{Im}\left[\frac{-1}{\varepsilon(k,\omega)}\right]_{\mathrm{outer}}+\mathrm{Im}\left[\frac{-1}{\varepsilon(k,\omega)}\right]_{\mathrm{inner}}\\&=\sum_i A_i\mathrm{Im}\left[\frac{-1}{\varepsilon_{\mathrm{M}}(\omega_i,\gamma_i;k=0,\omega)}\right]\Theta(\omega-\omega_{\mathrm{th},i})\\&\quad+\frac{2\pi^2\mathcal{N}}{\omega}\sum_{n\ell}\frac{\mathrm{d}f_{n\ell}(k,\omega)}{\mathrm{d}\omega}\end{aligned} \tag{5}$$

where, in order to include condensed target effects, the outer electron contribution to the ELF is fitted to the experimental optical ELF by a weighted sum of Mermin-type ELF (Mermin, 1970). In the above expression $\varepsilon_{\mathrm{M}}$ is the Mermin dielectric function, $A_i$, $\omega_i$ and $\gamma_i$ are, respectively, the intensity, position and width of each Mermin-type ELF, $\hbar\omega_{\mathrm{th},i}$ is a threshold energy; all these values are presented in Table 1 for the different materials discussed in this paper. The inner-shell electrons are described by their generalized oscillator strengths (GOS) in the hydrogenic approach, where $\mathrm{d}f_{n\ell}(k,\omega)/\mathrm{d}\omega$ is the GOS of the $(n,\ell)$ sub-shell and $N$ is the molecular density of the target. The recompense of this model is that if one fits the ELF to the experimental data at $k=0$, due to the analytical dependence of the Mermin dielectric function with the momentum transfer, it is not necessary to assume any extension algorithm to obtained the Bethe surface. Another important quantity that can be obtained with the MELF-GOS model is the mean excitation energy $I$ of the target, whose values are 79.4 for liquid water (Garcia-Molina et al., 2009),